Switching with vortex beams in nonlinear concentric couplers

José R. Salgueiro[1] **and Yuri S. Kivshar**[2]

[1]*Departamento de Física Aplicada, Universidade de Vigo, Facultade de Ciencias de Ourense, As Lagoas s/n, 32004 Ourense, Spain*
[2]*Nonlinear Physics Center, Research School of Physical Sciences and Engineering, Australian National University, ACT 0200 Canberra, Australia*

jrs@uvigo.es, ysk124@rsphysse.anu.edu.au

Abstract: We demonstrate that a concentric ring coupler can be employed for nonlinear switching of the angular momentum of light carried by an optical vortex. We find different types of stationary vortex states in the nonlinear coupler and study coupling of both power and momentum of an optical vortex launched into one of the rings, demonstrating that the switching takes place well below the collapse threshold. The switching is more effective for the inner-ring excitation since it triggers more sharply and for the powers low enough to avoid the vortex instability and breakup.

OCIS codes: (190.3270) Kerr effect; (060.1810) Buffers, couplers, routers, switches, and multiplexers

References and links

1. M. S. Soskin and M. V. Vasnetsov, "Singular optics," in *Progress in Optics*, E. Wolf, ed., vol. 42, p. 219 (North-Holand, Amsterdam, 2001).
2. A. S. Desyatnikov, Yu. S. Kivshar, and L. Torner, "Optical vortices and vortex solitons," in *Progress in Optics*, E. Wolf, ed., vol. 47, pp. 291–391 (North-Holand, Amsterdam, 2005).
3. Yu. S. Kivshar and G. P. Agrawal, *Optical Solitons: From Fibers to Photonic Crystals* (Academic Press, San Diego, 2003), 520 pp.
4. Y. V. Kartashov, V. A. Vysloukh, and L. Torner, "Rotary solitons in Bessel optical lattices," Phys. Rev. Lett. **93**, 093904-4 (2004).
5. X. Wang, Z. Chen, and P. G. Kevrekidis, "Observation of discrete solitons and soliton rotation in optically induced periodic ring lattices," Phys. Rev. Lett. **96**, 083,904 (2006).
6. Q. E. Hoq, P. G. Kevrekidis, D. J. Frantzeskakis, and B. A. Malomed, "Ring-shaped solitons in a dartboard photonic lattice," Phys. Lett. A **341**, 341–155 (2006).
7. L. Djaloshinski and M. Orenstein, "Disk and ring microcavity lasers and their concentric coupling," IEEE J. Quantum Electron. **35**(5), 737–744 (1999).
8. M. Heiblum and J. H. Harris, "Analysis of curved optical waveguides by conformal transformation," IEEE J. Quantum Electron. **11**, 75–83 (1975).
9. N. N. Akhmediev and A. Ankiewicz, *Solitons: Nonlinear Pulses and Beams* (Chapman & Hall, Cornwall, 1997).
10. J. F. Nye, *Natural Focusing and Fine Structure of Light: Caustics and Wave Dislocations* (Taylor & Francis, 1999).

1. Introduction

Optical vortices are fundamental structures in the light fields associated with the points of vanishing intensity and phase singularities of optical beams [1]. Optical vortices have been generated experimentally in different types of linear and nonlinear optical media [1, 2]. However, when a vortex beam propagates in a nonlinear medium, it becomes unstable due to the

#85524 - $15.00 USD Received 20 Jul 2007; revised 4 Sep 2007; accepted 18 Sep 2007; published 24 Sep 2007

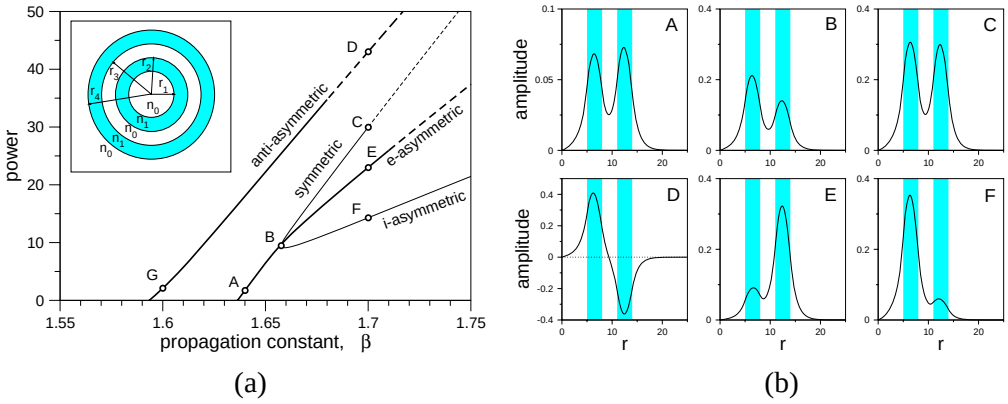

Fig. 1. (a) Power diagram of the ring nonlinear coupler. Dashed lines represent the unstable collapsing solutions. Inset: Sketch of the concentric ring coupler. Values used (in normalized units) are: $r_1 = 5$, $r_2 = 8$, $r_3 = 11$ and $r_4 = 14$ for radii and $n_0 = 1$, $n_1 = 2$ for indices. (b) Examples of nonlinear stationary states corresponding to the points marked on the power diagram (labels A to F are correspondent in both subfigures).

symmetry-breaking azimuthal instability [2] decaying into several fundamental solitons [3]. Therefore, it is commonly accepted that any kind of an optical device operating with a transfer of the angular momentum of light and realizing nonlinear switching of an optical vortex would be impossible due to this inherent nonlinear instability and the subsequent vortex decay.

In a contrast to this common belief, in this paper we suggest a novel type of nonlinear waveguide coupler created by two weakly coupled concentric ring waveguides which not only preserves the angular momentum of the input light during the propagation, but also allow *nonlinear switching* for the beam power and angular momentum operating with ring-like optical vortex beams. Such two-ring annular waveguide couplers can be created, in particular, by a proper modulation of nondiffracting ring Bessel-like optical lattices [4] recently generated experimentally by the optical induction technique [5]. In this context, the ring-shaped solitons were studied in a multi-ring lattice for the case of a saturable nonlinearity [6].

The purpose of this paper is twofold. First, we suggest a simple design of a concentric ring coupler that is consistent with the conservation of the angular momentum of the vortex beam. Second, we study the angular momentum switching in this coupler and compare it with the familiar switching of the fundamental beams. We are interested how an input beam with a nonzero angular momentum can tunnel between the ring-like cores (either from the outer ring or from the inner ring) of the annular coupler, in both linear and nonlinear regimes. To the best of our knowledge, this problem has never been addressed before, but it seems very important for suggesting novel ways to manipulate, transform, and control the angular momentum of light.

2. Model and stationary states

We consider a pair of two concentric step-index ring waveguides shown in the inset of Fig. 1(a). The two concentric cores and the substrate are made of two different materials with the refractive indices n_1 and n_0, and both possessing a nonlinear Kerr response. For the sake of simplicity, we took $n_0 = 1$ (base index) and $n_1 = 2$ (so that the index difference is $\Delta n = 1$) in all our calculations. The study is, however, valid for any other values of the indices, since changing the index difference only supposes a change in the spatial scale of the system and a change in the base index only produces a shift in the propagation constants. The scalar optical field $\psi(r,\phi,z)$

#85524 - $15.00 USD Received 20 Jul 2007; revised 4 Sep 2007; accepted 18 Sep 2007; published 24 Sep 2007

propagating in the z-direction may be described by the normalized equation,

$$i\frac{\partial\psi}{\partial z}+\nabla_{\perp}^{2}\psi+\left[V(r)+|\psi|^{2}\right]\psi=0, \tag{1}$$

where $\nabla_{\perp}^{2}$ is the Laplace operator, and $V(r)$ is the external potential of the double-ring coupler. In the linear regime, this kind of annular structures were studied by means of a conformal transformation [7, 8], although in a nonlinear regime a numerical approach is more directly applicable. Since we are interested in ring-shaped fields with nonzero angular momentum, the indices and dimensions of the coupler are chosen such that the linear coupler supports the usual even and odd (respect to the middle point between both cores) vortex-type modes. Also, each of the waveguides, when considered separately, supports the lowest-order vortex-type mode.

We look for the stationary states of the model (1) in the form,

$$\psi(r,\phi,z)=u(r)\exp(i\ell\phi)\exp(i\beta z), \tag{2}$$

where $u(r)$ is the radial profile of the corresponding stationary state, β is its propagation constant, and ℓ is the winding number. Substitution of this function into the model (1) yields to the following z-independent equation,

$$-\beta u+\frac{d^{2}u}{dr^{2}}+\frac{1}{r}\frac{du}{dr}-\frac{\ell^{2}u}{r^{2}}+\left[V(r)+u^{2}\right]u=0. \tag{3}$$

We consider, for the sake of simplicity, the lower states with nonzero angular momentum, when $\ell=1$. The nonlinear stationary states can be calculated numerically, and they are characterized by the power $P=2\pi\int u^{2}r\,dr$ as a function of the propagation constant β, as shown in the power diagram of Fig. 1(a). Examples of the nonlinear stationary states corresponding to different points in the power diagram are shown in Fig. 1(b). Due to the inherent asymmetry of the coupler, at low powers there exist two branches represented by asymmetric modes, one even with power concentrated on the external ring (*e-asymmetric*), and one odd (regarded as *anti-asymmetric*), whose limit at $P=0$ correspond to the linear modes of the concentric ring coupler. When power exceeds a particular threshold, there appear two new branches, one *symmetric* and another asymmetric with power concentrated on the internal ring (*i-asymmetric*) which join together at point B. The point B is out of the e-asymmetric branch due to asymmetry of the coupler which remove degeneracy of the bifurcation point of a symmetric nonlinear coupler [9].

Stability of nonlinear states depends on the branch symmetry and power [9]. In general, in our case all nonlinear states develop an azimuthal instability if they propagate for a long enough distance, although those belonging to the e-symmetric and anti-asymmetric branches can be considered 'practically stable', if the mode power is low enough. As an example, the mode corresponding to point A (see Fig. 1(a)) breaks only for $z>25000$, while the mode G breaks at $z>6000$. Since the powers of those two states are similar, we conclude that e-asymmetric states are less favored to develop the azimuthal instability, remaining stable for much longer distances. Above the threshold where the symmetric and i-asymmetric states exist, the i-asymmetric states are less unstable: the mode F breaks at $z>200$ whereas the mode C breaks at $z>50$. For higher powers, all the modes become strongly unstable and they first break into a number of lobes, and then develop the collapse instability (dashed lines in Fig. 1(a)) as usual happens in self-focusing nonlinear Kerr media [3]. Due to the presence of the ring waveguides the beam spreading is stopped and so for low powers the beam remains stable.

3. Vortex switching

In order to study the coupling of power and angular momentum, we launch a vortex beam into one of the ring waveguides. We chose the initial vortex of the form of Eq. (2) with $\ell=1$, but

#85524 - $15.00 USD Received 20 Jul 2007; revised 4 Sep 2007; accepted 18 Sep 2007; published 24 Sep 2007

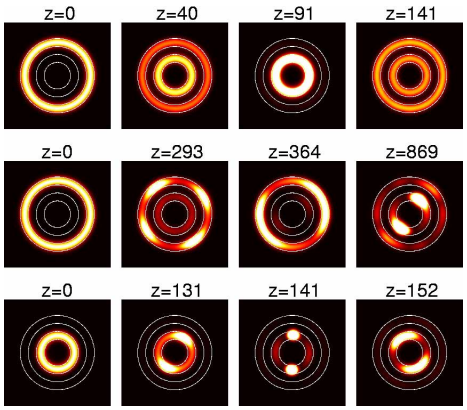

Fig. 2. Distribution of the light intensities in the coupler for different propagation distance z, for three different regimes. Top: external core excitation for the initial power $P = 5$. Center: external core excitation, at $P = 20$. Bottom: internal core excitation, at $P = 20$.

taking the radial shape of the field $u(r) = u_0(r)$ to be that of the single-waveguide mode in order to assure a good coupling to the ring waveguide, although there would be no problem to take some other shape like Gaussian. The field is also initially scaled to establish the desired power and then propagates in a nonlinear regime. At each value of z, we characterize the vortex beam by calculating the beam power, $P = \int |\psi|^2 \, r dr d\phi$, and the angular momentum, $L_z = \mathrm{Im}\{\int \psi^* \partial_\phi \psi \, r dr d\phi\}$, which are monitored for each waveguide. To do so, we consider a circular boundary just half way between both the cores and use all the points located in the inner part of this boundary to calculate the power and momentum for the inner core, and those in the external part to calculate those values for the external core.

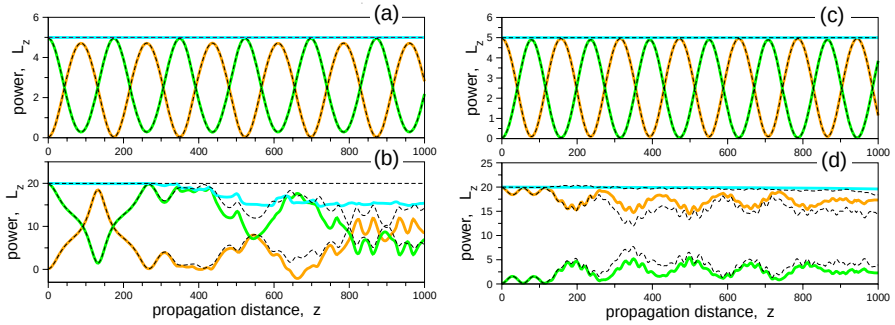

Fig. 3. Normalized power (dashed) and angular momentum (solid) vs. propagation distance for ring excitation with a single- charged vortex. The individual values for each core are plotted, together with the total values. (a) simulation for external-core excitation at P=5; (b) the same at P=20; (c) simulation for internal-core excitation at P=5; (d) the same at P=20.

In Fig. 2, we show the intensity images of the coupler for three different scenarios. Also, for both internal and external ring excitations, in Fig. 3, we plot the power and angular momentum for each waveguide together with their total values. Both magnitudes are in normalized units and on the same scale. In fact, according to the functional form of the input field $\psi_0(r,\phi) =$

#85524 - $15.00 USD Received 20 Jul 2007; revised 4 Sep 2007; accepted 18 Sep 2007; published 24 Sep 2007

$u_0(r)\exp(i\ell\phi)$, they are initially proportional,

$$L_z = \mathrm{Im}\left\{\int \psi_0^* \partial_\phi \psi_0 \, r\, dr\, d\phi\right\} = 2\pi\ell \int u_0(r)^2 r dr = \ell P. \tag{4}$$

The top row in Fig. 2 shows the case when the external core of the ring coupler is excited with a low-power vortex beam. A periodic power and momentum transfer between the cores is observed, and the beam remains stable. At such low powers, a similar result is obtained when the inner core of the coupler is excited. If the power is increased (center row), the azimuthal instability breaks the beam into a number of the fundamental solitons after some propagation distance. The larger the input power the shorter the propagation distance at which the vortex breakup occurs. The resulting fundamental solitons have an oscillating width, and they rotate inside the ring due to the initially imposed angular momentum, with an angular velocity that is larger as the solitons width is smaller (see the movies). If the input power is further increased, the fundamental solitons collapse.

Due to the proportionality relationship between the momentum and power [see Eq. (4)], and the fact that we chose $\ell = 1$, the power and angular momentum have the same numerical value meanwhile the beams remain unbroken (notice coincident continuous and dashed lines in Fig. 3). Nevertheless, it is notable that this parallel behavior diverges from the point where the beams breakup occurs, due to the instabilities (notice a separation of the continuous and dashed lines), revealing differences in the momentum coupling. Besides, the total angular momentum is not longer conserved as is shown in the plots.

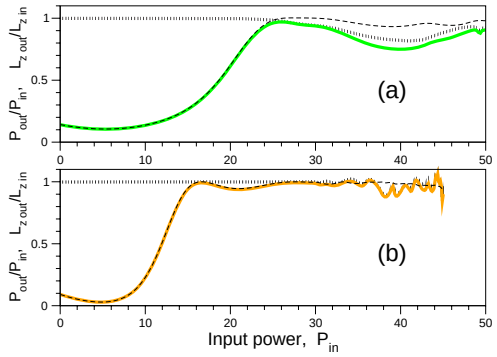

Fig. 4. Switching curves for the power (dark dashed lines) and angular momentum (light continuous lines) for (a) outer-waveguide excitation, and (b) inner-waveguide excitation. Also shown is the total angular momentum (dotted line).

Another interesting feature observed in simulations is the difference in suppression of coupling between internal and external ring excitation. When the larger external-ring core is excited, a higher power density is coupled into the inner core, and the beam breaks for a lower input power than the necessary to complete the switching. This is evident from Fig. 2 (center row) where it is shown that after the beam breakup, the core coupling is still possible for a long enough propagation distance. To account for the switching property, in Fig. 4 we show the switching curves for both vortex power and angular momentum. They are constructed by launching the field into one of the cores, simulating the propagation for half a beating length and measuring the output power at the same core; the plot is the ratio between output and input power. The beating length is defined as the distance required to perform a complete coupling cycle, i.e. a power transfer to the second core and back to the first core, and it is obtained by simulation in the linear regime. For the parameter values considered here the half beating length resulted in z=73.75 and z=73.85, for internal and external ring excitation, respectively.

#85524 - $15.00 USD Received 20 Jul 2007; revised 4 Sep 2007; accepted 18 Sep 2007; published 24 Sep 2007

We mention also that, due to the asymmetry of the coupler (i.e., the rings of different diameters), a complete power transfer does not occur in the linear regime. That is why raising the power produces an initial increase of the coupled power and the switching curve decreases at low powers. Also, for the external-ring excitation, see Fig. 4(a), the triggering is more steady and it takes place at higher powers than that for the internal-ring excitation, Fig. 4(b). This is due to a lower power density in the external ring because of its larger area. The power diagram of Fig. 1(a) allows to explain the switching property. In fact, for powers over the threshold (power around that of point B), the existence of both asymmetric modes with a lower power and higher stability than the symmetric one makes the energy to remain in the first excited core.

The separation between the power and angular momentum curves denotes the point where the azimuthal instability breaks the beam before it propagates half a beating length. It happens clearly after switching takes place in the case of internal-ring excitation, but slightly below that point, for external-ring excitation. This behavior is consistent with the fact that the i-asymmetric branch in the power diagram of Fig. 1(a) is more stable than the e-asymmetric one. The curves reach an end-point when the power is so high that collapse takes place before the beam propagates for half a beating length. This fact, together with the higher slope of the switching curve makes internal-ring excitation more effective for both power and angular momentum switching.

A practical implementation of the device could be carried out in a number of ways, for instance by a omnidirectional optical waveguide. Another possibility is the use of the optical induction technique, for example illuminating a photorefractive crystal with the suitable pattern to generate the coupler. The basic requirements are that the coupler waveguides support the lowest vortex mode and the materials are able to show the nonlinear effects for the power used.

Finally, we would like to mention briefly our studies of the structural stability of the vortex switching. It is known [10] that singularities in systems with some artificial symmetry features are nongeneric, i.e. they may become structurally unstable. In the system we have studied here, it is assumed that the axes of both the waveguide and launched vortex beam coincide ideally, while in a practical implementation they would present nonvanishing errors. In this way, we have performed a series of additional simulations when the center of the launched vortex is transversally shifted. We have observed that the instabilities appear for shorter propagation distances, and this distance decreases dramatically for a small shift, but after a further increase of the shift it saturates, affecting the switching much weaker. On the other hand, such instabilities for the inner excitation do not appear in the first coupling period, even for moderately large displacements. This still allows the vortex switching to occur without azimuthal instabilities. Finally, the larger the shift the larger the amount of power which is dissipated due to the coupling mismatch. In summary, we have found that the effect of the shift is quantitative, and it does not change substantially any of the results presented above.

4. Conclusions

We have suggested a ring optical coupler for periodic transfer of both power and angular momentum of light. In the nonlinear regime, we demonstrate that the internal-ring excitation is more effective since the slope of the switching curve is larger and switching is triggered well before the vortex beam breaks up due to the azimuthal instability. A study of the structural instabilities demonstrated the usefulness of the device under realistic practical conditions.

Acknowledgments

JRS acknowledges the Ramón y Cajal contract from the Ministerio de Educación y Ciencia of Spain and a support from Xunta de Galicia (project PGIDIG06PXIB239155PR). YK acknowledges a support from the Australian Research Council and discussions with A. Desyatnikov.

#85524 - $15.00 USD Received 20 Jul 2007; revised 4 Sep 2007; accepted 18 Sep 2007; published 24 Sep 2007